JOURNAL OF COMPUTATIONAL PHYSICS **144,** 137–150 (1998)
ARTICLE NO. CP985985

A Discrete Model for the Lightning Discharge

William W. Hager

Department of Mathematics and Center for Applied Optimization,
University of Florida, Gainesville, Florida 32611
E-mail: hager@math.ufl.edu

Received August 28, 1997; revised March 24, 1998

For a lightning discharge model presented by the author, J. S. Nisbet, and J. R. Kasha (*J. Comput. Phys*, **82**, 193, 1989), we simulate lightning by letting the conductivity tend to infinity wherever the electric field reaches the breakdown threshold. Here we show that for this discharge model and for a one parameter family of integration schemes, the backward Euler scheme is the only one that leads to the equilibration of the electric potential along the discharge channel. Moreover, the potential obtained by letting the conductivity tend to infinity in the continuous equation is identical to the potential obtained in the backward Euler approximation when conductivity tends to infinity. Connections to diffusion limited aggregation (DLA), to more recent schemes for simulating the lightning discharge, and to experiments of Williams *et al.* are discussed.

1. INTRODUCTION

In a series of papers [2–4], we developed a method to simulate a lightning discharge. A flash was initiated when the electric field reached the so-called "breakdown threshold." The model generated the discharge region, charge transfer, and detailed charge rearrangement associated with the flash. The model was obtained by discretizing Maxwell's equations using volume elements in space, and a backward Euler scheme in time, and then evaluating the solution limit as the conductivity tends to infinity in the breakdown region. In this paper we focus on the time integration, and we show that if time evolves continuously, without any discretization, we obtain precisely the same formulas for the discharge process that were obtained earlier using the backward Euler scheme. Hence, even though a temporal discretization appeared in our earlier work, the formula we obtained was exact in the sense that it coincides with the formula associated with the continuous time process.

In our earlier work, we chose the backward Euler time scheme based on the following physical consideration: A cloud discharge should equilibrate the electric potential along the discharge channel. When one considers a one parameter family of integration schemes that includes the backward Euler (implicit) scheme and the forward Euler (explicit) scheme, the

0021-9991/98 $25.00

backward Euler scheme is the only member of the family that equilibrates of the electric potential along the discharge channel. Hence, the discretization used in our earlier work based on physical considerations, now has a rigorous mathematical basis as well since it generates the electric potential obtained by exact integration of the equations of evolution.

We now discuss the relation between our lightning discharge scheme and both earlier and later work. There are some connections with the theory of "diffusion limited aggregation" or DLA (we thank Sergei Obukhov for pointing out this possible connection). One of the first papers [20] in this area appeared in 1981, and subsequently, there has been enormous interest. Research into DLA has connections to fractals, to fractal dimension, to real-space renormalization group analysis, and to many other topics. One aspect of this DLA work, stochastic models for dielectric breakdown (see [11, 14]), is especially relevant to the lightning discharge. These stochastic models for dielectric breakdown arise out of an effort to model the complicated branching patterns that result from dielectric breakdown of gaseous, liquid, and solid insulators. Consider a lattice in 2 dimensions where the potential ϕ at the origin is fixed at zero while ϕ on a surrounding circle is held fixed at one. In [14] they think of the discharge process as corresponding to a series of bonds formed between adjacent lattice points with all bonded lattice points having potential zero. The bonds grow in a stochastic, stepwise fashion, starting from the origin. In any step, we first solve Laplace's equation in the circular domain subject to the boundary conditions that ϕ is one on the surrounding circle, while ϕ is zero on the bonded set. We connect a new bond to the existing bonded set where the probability of bonding (i, j) to an adjacent lattice point (i', j') is in proportion to $\phi(i', j')^\eta$. Here $\eta > 0$ is a fixed parameter associated with the discharge process—η can be varied in order to try to make the modeled discharge resemble experimentally observed discharges. Since (i', j') is adjacent to (i, j) in the lattice and since $\phi(i', j') - \phi(i, j) = \phi(i', j')$, it follows that $\phi(i', j')$ approximates either $\phi_x(i, j)$ or $\phi_y(i, j)$; that is, $\phi(i', j')$ approximates either the x or y component of the electric field at the lattice point (i, j). Hence, if the likelihood of a new bond is proportional to $\phi(i', j')^\eta$, then loosely speaking, the most likely bonds to form are those where the local electric field is largest. There has been much follow-up work on this strategy for modeling dielectric breakdown, including application to ball lightning [16], computation of the fractal dimension of lightning using digitized pictures [15], and some simulations of two dimensional cloud discharges [13].

In comparing this DLA discharge approach to our discharge scheme, the approaches are related in the sense that Laplace's equation enters into the model and discharge branches tend to form where the electric fields are largest. On the other hand, there are fundamental differences. There are no unknown parameters like η in our scheme, our scheme is deterministic not stochastic, and in our scheme, we do not need to know the potential at a point in the middle of the domain (recall the assumption that ϕ is zero at the origin of the lattice, and along the bonded set). In our approach, we only require boundary conditions on the outside of the domain, and everywhere inside the domain, including the breakdown region itself, we compute the potential. In the literature on dielectric breakdown, the prevalent view seems to be that since the observed breakdown regions are complex and tortuous with many branches, the underlying physical processes are stochastic in nature. In contrast, in our approach, we obtain similar complex, branched structures in an entirely deterministic fashion in which the branching is caused by activation of the constraint $|\mathbf{E}| = |\nabla\phi| \leq$ breakdown threshold, when we solve the associated Maxwell's equations.

Laboratory experiments seem to confirm the important role played by the static electric field in discharge propagation. In a fascinating paper [19], Williams, Cooke, and Wright,

develop an *experimental* model for cloud discharges using a dielectric material polymethylmethacrylate. They state, "Despite the complications imposed by the geometry of the developing discharge in charged clouds, all the laboratory results in this study indicate that the discharge is controlled predominately by a single parameter: the local electrostatic field. It is a knowledge of this local field response that is essential in determining how discharges propagate in and around arbitrary distributions in space charge." We return to this observation later.

Two other discharge models appeared in the literature more recently. In the model of Helsdon, Wu, and Farley (see [7, 8, 17]) lightning propagates along the electric field lines, starting from a point where the electric field first reaches the breakdown threshold. The ends of the channel are the first points along the propagation path where the magnitude of the electric field is less than the termination criterion (150 kV/m). It is assumed that the linear charge density at any point P along the channel is proportional to the difference between the potential at the point where the discharge emanates, and the potential at P. The value of this proportionality constant κ controls the amount of charge transferred by the discharge. In order to maintain charge neutrality over the channel, it is extended by four grid points beyond the designated termination point. In this extended region, it is assumed that the charge density drops off like $e^{-\alpha x^2}$, while a similar exponential decay of charge occurs around the channel.

In comparing this approach to our approach to cloud discharges, we note that branching cannot occur in their method. Their discharge simply follows the electric field lines until the termination condition is satisfied. (Note that a more recent paper [17] by Solomon and Baker gives a modification that allows a longer discharge path that can reach the earth). Observe that in the approach of [7, 8], there are many unknown parameters and assumptions that need physical justification.

In a different approach to lightning discharge, Ziegler and MacGorman [21] perform a charge rearrangement whenever the magnitude of the electric field exceeds the breakdown threshold. In any given time step, they determine the part of the model domain where the electric field exceeds the breakdown threshold, and throughout this region, they adjust the charge wherever the charge density exceeds a prescribed threshold. The amount of charge adjustment is proportional to the difference between the prescribed threshold and the local charge density. This approach leads to breakdown volumes, and is quite different from our approach.

2. THE DISCRETE EQUATIONS AND AN ELEMENTARY ARC BREAKDOWN

As explained in [4], our model for the lightning discharge involves the following assumptions:

(a) The time derivative of the magnetic field can be neglected.

(b) The electric field magnitude is always less than or equal to the breakdown threshold E_B.

(c) When the electric field reaches the breakdown threshold E_B at some point, the conductivity tends to infinity in a small neighborhood of that point.

Although in the numerical simulation of [4] we used a constant value 250 kV/m for E_B, we could just as easily have allowed E_B to depend on position. Moreover, recent experimental results by Marshall *et al.* [9, 10] indicate that the breakdown threshold in a thundercloud

may be even less than 250 kV/m. That is, when balloons fly through thunderstorms, electric field values greater than 150 kV/m are rarely detected. Hence, breakdown must occur at values of the electric field smaller than this. In [9] this smaller than expected value for the breakdown threshold is explained by the initiation of an electron avalanche.

Note that in a neighborhood of a lightning channel, assumption (a) is clearly not satisfied, and as a result, in the framework (a)–(c), we can never obtain the myriad of lightning phenomena (darts, M-components, J- and K-processes, multiple strokes along the same channel) described, for example, in the book [18] by Uman. Nonetheless, one is able to obtain the lightning channel and the charge rearrangement associated with a discharge. This information, when incorporated in thunderstorm models (e.g., see [5, 6, 12, 21, 22]) that describe the generation, interaction, and motion of charged particles, can be used to study the long-term evolution of a thunderstorm.

We emphasize that our simulation process yields the discharge region and the charge rearrangement, but not the speed of lightning or the number of return strokes. Roughly speaking, our simulation process can be described in the following way: We let the electric potential ϕ evolve according to Maxwell's equations, stopping at the first instant of time where the magnitude of $\nabla\phi$ reaches E_B. Letting the conductivity σ tend to infinity in a neighborhood of that point, ϕ is reevaluated by taking the limit in the equation of evolution. If the magnitude of $\nabla\phi$ is beneath E_B everywhere in the domain, we stop the lightning discharge. But in some cases, as σ tends to infinity, the magnitude of $\nabla\phi$ reaches E_B at a nearby point. When this happens, we let σ tend to infinity in a neighborhood of that nearby point. This process of repeatedly letting σ tend to infinity and checking the magnitude of $\nabla\phi$ continues until the magnitude of $\nabla\phi$ is beneath E_B everywhere in the domain. Although this breakdown process requires a number of steps as we successively let σ tend to infinity and reevaluate ϕ, we view the entire process as occurring instantly. As a result, we cannot determine the speed of lightning or the number of return strokes. Instead, we obtain the lightning channel, which we consider to be infinitesimally thin, and the charge rearrangement associated with the lightning.

Our breakdown model is based on Maxwell's equations. In particular, by Ampere's Law we have

$$\nabla \times \mathbf{H} = \varepsilon \frac{\partial \mathbf{E}}{\partial t} + \sigma \mathbf{E} + \mathbf{J}, \tag{1}$$

where ε is the permittivity, σ is the conductivity, $\mathbf{E}$ is the electric field, $\mathbf{J}$ is the current density associated with charged particles circulating in the cloud, $\sigma\mathbf{E}$ is the conduction current density, and $\varepsilon\frac{\partial \mathbf{E}}{\partial t}$ is the displacement current density. We assume that $\mathbf{J}$ is known and that we wish to solve for the electric field. Taking the divergence gives

$$\varepsilon \nabla \cdot \frac{\partial \mathbf{E}}{\partial t} + \nabla \cdot \sigma \mathbf{E} + \nabla \cdot \mathbf{J} = 0. \tag{2}$$

By assumption (a), $\nabla \times \mathbf{E} = \mathbf{0}$, $\mathbf{E}$ is the gradient of a potential ϕ, and (2) yields

$$\varepsilon \frac{\partial \nabla^2 \phi}{\partial t} + \nabla \cdot (\sigma \nabla \phi) + \nabla \cdot \mathbf{J} = 0, \tag{3}$$

where ∇^2 denotes the Laplacian operator defined by $\nabla^2 = \nabla \cdot \nabla$.

To discretize (3), we integrate over volume elements, and then we replace gradients by finite differences. Although there are many ways to carry out the discretization process, this approach leads to a system of differential equations for which we can analyze the effect of letting σ tend to infinity at a point in space where the magnitude of the electric field is equal to the breakdown threshold. To simplify the discussion, suppose that the region of interest is decomposed into cubes with the sides of the cubes parallel to the axes of a Cartesian coordinate system. Integrating (3) over each cube, applying the divergence theorem, and interchanging the order of differentiation, we obtain the following relation for a typical cube C in the tessellation,

$$\int_{\partial C} \varepsilon \nabla \frac{\partial \phi}{\partial t} \cdot \mathbf{dS} + \int_{\partial C} \sigma \nabla \phi \cdot \mathbf{dS} + i = 0, \tag{4}$$

where i is the net current leaving C and ∂C is the boundary of C.

If $\mathbf{\Phi}$ is a vector whose components are the values of the potential at the centroid of each cube, then $\nabla \frac{\partial \phi}{\partial t} \cdot \mathbf{dS}$ on a face of a cube is approximated by the area of the face times the difference between the values of $\frac{\partial \phi}{\partial t}$ at the centroid of the cubes on opposite sides of the face, divided by the distance between the centroids. A similar approximation can be used for the $\nabla \phi \cdot \mathbf{dS}$ term in (4) except that we multiply by the value of σ at the centroid of each face. With these finite difference approximations, we arrive at an equation of the form

$$\mathbf{A}\dot{\mathbf{\Phi}} + \mathbf{B}\mathbf{\Phi} + \mathbf{i} = 0, \tag{5}$$

where the dot above $\mathbf{\Phi}$ denotes time derivative. The matrix $\mathbf{A}$ obtained by this process is essentially a discretization of the Laplacian operator ∇^2. The structure of $\mathbf{B}$ is similar except that it involves the values of σ at the centroids of each face (see [3] for the details).

To implement the constraint $\|\mathbf{E}\| \le \mathbf{E}_B$ given in (b) on the Euclidean length of $\mathbf{E}$, we employ the more tractable sup-norm constraint $\|\mathbf{E}\|_\infty \le \mathbf{E}_B$ where

$$\|\mathbf{E}\|_\infty = \text{maximum}\{|E_x|, |E_y|, |E_z|\}.$$

In particular, for the discretization (5) where $\mathbf{\Phi}$ is the vector whose components are the potential at the centroid of each cube, let $\Phi_a(t)$ and $\Phi_b(t)$ denote the potential at the centroids of two adjacent cubes in the tessellation. We approximate the condition $\|\mathbf{E}(t)\|_\infty \le E_B$ by the finite difference relation

$$\frac{|\Phi_a(t) - \Phi_b(t)|}{h} \le E_B, \tag{6}$$

where h is the centroid separation. The condition (6) must be satisfied for each pair of components of $\mathbf{\Phi}$ associated with adjacent cubes. At any instant of time where (6) becomes an equality for an index pair (j, k) associated with a pair of adjacent centroids in the tessellation, we let the value of σ on the associated cube face tend to infinity. As we change the value of σ on this face, Eq. (5) is transformed to

$$\mathbf{A}\dot{\mathbf{\Phi}} + (\mathbf{B} + \tau \mathbf{w}\mathbf{w}^T)\mathbf{\Phi} + \mathbf{i} = 0, \tag{7}$$

where τ is proportional to the difference between the new (large) value for σ and the original value, the superscript T denotes transpose, and $\mathbf{w}$ is a vector whose entries are all zero except that $w_j = 1$ and $w_k = -1$.

In order to evaluate the effect of this breakdown of the atmosphere (corresponding to letting σ, or equivalently τ, tend to infinity), we need to evaluate the solution to (7) at an instant of time, t^+, just beyond t, as τ tends to infinity. In our earlier work [2, 3], we analyzed this limit when (7) was approximated by the backward Euler time discretization. This backward Euler approximation was the basis for the simulations [4] in which we compared the fields of the model to observed electric fields.

3. A ONE PARAMETER FAMILY OF INTEGRATION SCHEMES

Letting μ be a parameter, let us consider the following one parameter family of integration schemes associated with (5):

$$\mathbf{A}[\mathbf{\Phi}^{n+1} - \mathbf{\Phi}^n] + \Delta t \mathbf{B}[\mu \mathbf{\Phi}^{n+1} + (1-\mu)\mathbf{\Phi}^n] = \Delta t \mathbf{i}^n. \tag{8}$$

In [3] we note that the discretization process described above leads to symmetric matrices $\mathbf{A}$ and $\mathbf{B}$ that are positive definite when the electric potential vanishes on the boundary of the problem domain, and in this case, (8) is unconditionally stable for $\mu \geq 1/2$, while it is conditionally stable (Δt should be sufficiently small) for $\mu < 1/2$. In [4] we observe that the Crank–Nicholson scheme ($\mu = 1/2$) produced the best accuracy in time integration up to a flash.

Let us now apply this scheme to (7) and examine the limit as τ tends to infinity and as Δt tends to zero. That is, if $\mathbf{\Phi}^n(\Delta t, \tau)$ is the solution $\mathbf{\Phi}^{n+1}$ to

$$\mathbf{A}[\mathbf{\Phi}^{n+1} - \mathbf{\Phi}^n] + \Delta t (\mathbf{B} + \tau \mathbf{w}\mathbf{w}^T)[\mu \mathbf{\Phi}^{n+1} + (1-\mu)\mathbf{\Phi}^n] = \Delta t \mathbf{i}^n, \tag{9}$$

we wish to evaluate the limit, denoted $\mathbf{\Phi}^{n+}$, given by

$$\mathbf{\Phi}^{n+} = \lim_{\Delta t \to 0} \lim_{\tau \to \infty} \mathbf{\Phi}^n(\Delta t, \tau).$$

THEOREM 1. *If* $\mathbf{A}$ *and* $\mathbf{B}$ *are symmetric and* $\mathbf{A}$ *is positive definite, then*

$$\mathbf{\Phi}^{n+} = \mathbf{\Phi}^n - \frac{1}{\mu} \frac{\mathbf{w}^T \mathbf{\Phi}^n}{\mathbf{w}^T \mathbf{A}^{-1} \mathbf{w}} \mathbf{A}^{-1} \mathbf{w}. \tag{10}$$

Moreover, we have

$$\Phi_j^{n+} - \Phi_k^{n+} = \left(1 - \frac{1}{\mu}\right)\left(\Phi_j^n - \Phi_k^n\right). \tag{11}$$

Proof. Rearranging (9) gives

$$(\mathbf{A} + \Delta t \mu (\mathbf{B} + \tau \mathbf{w}\mathbf{w}^T))\mathbf{\Phi}^{n+1} = (\mathbf{A} + (\mu - 1)\Delta t (\mathbf{B} + \tau \mathbf{w}\mathbf{w}^T))\mathbf{\Phi}^n + \Delta t \mathbf{i}^n. \tag{12}$$

Let us define the matrix $\mathbf{C}(\Delta t) = \mathbf{A} + \Delta t \mu \mathbf{B}$, and the quantity $\rho = \Delta t \mu \tau$. Hence, the coefficient matrix for $\mathbf{\Phi}^{n+1}$ in (12) has the form $\mathbf{C}(\Delta t) + \rho \mathbf{w}\mathbf{w}^T$. Since $\mathbf{A}$ is positive definite and $\mathbf{B}$ is symmetric $\mathbf{C}(\Delta t)$ is positive definite for Δt sufficiently small. Since $\rho > 0$, it follows that $\mathbf{C}(\Delta t) + \rho \mathbf{w}\mathbf{w}^T$ is also positive definite (for Δt sufficiently small). By

the Sherman–Morrison–Woodbury formula (see [2]), the inverse of the coefficient matrix can be expressed as

$$(\mathbf{C}(\Delta t)+\rho\mathbf{w}\mathbf{w}^T)^{-1}=\mathbf{C}(\Delta t)^{-1}-\frac{\rho}{1+\rho\mathbf{w}^T\mathbf{C}(\Delta t)^{-1}\mathbf{w}}\mathbf{C}(\Delta t)^{-1}\mathbf{w}\mathbf{w}^T\mathbf{C}(\Delta t)^{-1}. \quad (13)$$

Hence, as ρ tends to infinity (or equivalently, as τ tends to infinity), we have

$$\lim_{\rho\to\infty}(\mathbf{C}(\Delta t)+\rho\mathbf{w}\mathbf{w}^T)^{-1}=\mathbf{C}(\Delta t)^{-1}-\frac{\mathbf{C}(\Delta t)^{-1}\mathbf{w}\mathbf{w}^T\mathbf{C}(\Delta t)^{-1}}{\mathbf{w}^T\mathbf{C}(\Delta t)^{-1}\mathbf{w}}.$$

Note too that as Δt tends to zero, $\mathbf{C}(\Delta t)$ approaches $\mathbf{A}$, and since $\mathbf{A}$ is invertible, $\mathbf{C}(\Delta t)^{-1}$ approaches $\mathbf{A}^{-1}$. It follows from (9) that $\mathbf{\Phi}^{n+}$ is the sum of the following terms denoted Eqs. (14)–(16):

$$\lim_{\Delta t\to 0}\lim_{\rho\to\infty}\Delta t(\mathbf{C}(\Delta t)+\rho\mathbf{w}\mathbf{w}^T))^{-1}((\mu-1)\mathbf{B}\mathbf{\Phi}^n+\mathbf{i}^n)$$
$$=\left[\mathbf{A}^{-1}-\frac{\mathbf{A}^{-1}\mathbf{w}\mathbf{w}^T\mathbf{A}^{-1}}{\mathbf{w}^T\mathbf{A}^{-1}\mathbf{w}}\right]\lim_{\Delta t\to 0}\Delta t((\mu-1)\mathbf{B}\mathbf{\Phi}^n+\mathbf{i}^n)=0, \quad (14)$$

$$\lim_{\Delta t\to 0}\lim_{\rho\to\infty}(\mathbf{C}(\Delta t)+\rho\mathbf{w}\mathbf{w}^T))^{-1}\mathbf{A}\mathbf{\Phi}^n$$
$$=\left[\mathbf{A}^{-1}-\frac{\mathbf{A}^{-1}\mathbf{w}\mathbf{w}^T\mathbf{A}^{-1}}{\mathbf{w}^T\mathbf{A}^{-1}\mathbf{w}}\right]\mathbf{A}\mathbf{\Phi}^n=\mathbf{\Phi}^n-\frac{\mathbf{w}^T\mathbf{\Phi}^n}{\mathbf{w}^T\mathbf{A}^{-1}\mathbf{w}}\mathbf{A}^{-1}\mathbf{w}, \quad (15)$$

$$\lim_{\Delta t\to 0}\lim_{\tau\to\infty}(\mathbf{C}(\Delta t)+\Delta t\mu\tau\mathbf{w}\mathbf{w}^T))^{-1}\mathbf{w}\mathbf{w}^T\mathbf{\Phi}^n(\mu-1)\Delta t\tau. \quad (16)$$

To simplify (16), we apply (13) to obtain

$$(\mathbf{C}(\Delta t)+\rho\mathbf{w}\mathbf{w}^T)^{-1}\mathbf{w}=\frac{1}{1+\rho\mathbf{w}^T\mathbf{C}(\Delta t)^{-1}\mathbf{w}}\mathbf{C}(\Delta t)^{-1}\mathbf{w},$$

and (16) simplifies to

$$\lim_{\Delta t\to 0}\lim_{\tau\to\infty}\frac{(\mu-1)\Delta t\tau\mathbf{w}^T\mathbf{\Phi}^n}{1+\Delta t\mu\tau\mathbf{w}^T\mathbf{C}(\Delta t)^{-1}\mathbf{w}}\mathbf{C}(\Delta t)^{-1}\mathbf{w}=\frac{\mu-1}{\mu}\frac{\mathbf{w}^T\mathbf{\Phi}^n}{\mathbf{w}^T\mathbf{A}^{-1}\mathbf{w}}\mathbf{A}^{-1}\mathbf{w}. \quad (17)$$

Combining (14)–(17) yields (10). Taking the dot product of (10) with $\mathbf{w}$ and taking into account the fact that $w_j=1$ and $w_k=-1$, the proof is complete. ∎

Since we only let σ tend to infinity on the face of a cube where the left side of (6) is sufficiently large, the difference $\Phi_j^n-\Phi_k^n$ in (11) is never zero. It follows that the limit $\mathbf{\Phi}^{n+}$ of the potential depends on the choice of the parameter μ. The dependence of the limit on μ is troubling since one would like to see the potential converge to the same value (independent of μ) as the discretization parameters (the size of the cubes and the size of the time step Δt) tend to zero. In our earlier papers, we simply focused on the backward Euler time discretization ($\mu=1$). Our rationale for this choice of μ was based on the following physical consideration: The discharge process should equilibrate the potential along the discharge channel, and hence, the effect of a discharge should be to make Φ_j^{n+} equal to Φ_k^{n+}. By Theorem 1, the only value of μ that leads to the equilibration of the potential is $\mu=1$. In the next section, we observe that the expression (6) for the potential in the case $\mu=1$ is the exact limit of the differential equation (7) as τ tends to infinity.

4. THE CONTINUOUS LIMIT

We now examine the continuous limit in (7) as τ tends to infinity.

THEOREM 2. *If* $\mathbf{A}$ *is a positive definite matrix and* $\mathbf{\Phi}(t,\tau)$ *denotes the solution to* (7) *starting from the initial condition* $\mathbf{\Phi}(t_n,\tau)=\mathbf{\Phi}^n$, *then we have*

$$\lim_{\Delta t\to 0}\lim_{\tau\to\infty}\mathbf{\Phi}(t_n+\Delta t,\tau)=\mathbf{\Phi}^n-\mathbf{A}^{-1}\mathbf{w}(\mathbf{w}^T\mathbf{A}^{-1}\mathbf{w})^{-1}\mathbf{w}^T\mathbf{\Phi}^n. \tag{18}$$

Proof. For convenience, we set $t_n=0$ and we suppress the τ argument in $\mathbf{\Phi}(t,\tau)$. By the classic formula for the solution to a first-order system of differential equations, we have

$$\mathbf{\Phi}(\Delta t)=e^{-\mathbf{M}\Delta t}\mathbf{\Phi}^n-\int_0^{\Delta t}e^{-\mathbf{M}(\Delta t-s)}\mathbf{A}^{-1}\mathbf{i}\,ds, \tag{19}$$

where $\mathbf{M}=\mathbf{A}^{-1}(\mathbf{B}+\tau\mathbf{w}\mathbf{w}^T)$. Substituting for $\mathbf{M}$ gives

$$e^{-\mathbf{M}\Delta t}=e^{-\mathbf{A}^{-1}\mathbf{B}\Delta t}e^{-\tau\mathbf{A}^{-1}\mathbf{w}\mathbf{w}^T\Delta t}.$$

Recall that if $\mathbf{P}$ is a square matrix, then a matrix exponential $e^{\mathbf{P}}$ can be expanded in a Taylor series:

$$e^{\mathbf{P}}=\mathbf{I}+\mathbf{P}+\frac{\mathbf{P}^2}{2!}+\frac{\mathbf{P}^3}{3!}+\cdots. \tag{20}$$

We apply this expansion to $\mathbf{P}=-\tau\mathbf{A}^{-1}\mathbf{w}\mathbf{w}^T\Delta t$. To facilitate the simplification of the resulting expression, we use the associative law for matrix multiplication to obtain

$$(\mathbf{A}^{-1}\mathbf{w}\mathbf{w}^T)^2=\mathbf{A}^{-1}\mathbf{w}\mathbf{w}^T\mathbf{A}^{-1}\mathbf{w}\mathbf{w}^T=\mathbf{A}^{-1}\mathbf{w}\mathbf{w}^T(\mathbf{w}^T\mathbf{A}^{-1}\mathbf{w}).$$

In general, we have

$$(\mathbf{A}^{-1}\mathbf{w}\mathbf{w}^T)^\kappa=\mathbf{A}^{-1}\mathbf{w}\mathbf{w}(\mathbf{w}^T\mathbf{A}^{-1}\mathbf{w})^{\kappa-1}=\frac{\mathbf{A}^{-1}\mathbf{w}\mathbf{w}^T}{\mathbf{w}^T\mathbf{A}^{-1}\mathbf{w}}(\mathbf{w}^T\mathbf{A}^{-1}\mathbf{w})^\kappa. \tag{21}$$

Combining (20) and (21) gives

$$\begin{aligned}
e^{-\tau\mathbf{A}^{-1}\mathbf{w}\mathbf{w}^T\Delta t}&=\mathbf{I}+\sum_{\kappa=1}^{\infty}\frac{(-\tau\mathbf{A}^{-1}\mathbf{w}\mathbf{w}^T\Delta t)^\kappa}{\kappa!}\\
&=\mathbf{I}+\frac{\mathbf{A}^{-1}\mathbf{w}\mathbf{w}^T}{\mathbf{w}^T\mathbf{A}\mathbf{w}}\sum_{\kappa=1}^{\infty}\frac{(-\tau(\mathbf{w}^T\mathbf{A}^{-1}\mathbf{w})\Delta t)^\kappa}{\kappa!}\\
&=\mathbf{I}+\frac{\mathbf{A}^{-1}\mathbf{w}\mathbf{w}^T}{\mathbf{w}^T\mathbf{A}\mathbf{w}}\left(e^{-\tau(\mathbf{w}^T\mathbf{A}^{-1}\mathbf{w})\Delta t}-1\right).
\end{aligned}$$

Since $\mathbf{A}$ is positive definite, $\mathbf{w}^T\mathbf{A}^{-1}\mathbf{w}>0$, and $e^{-\tau(\mathbf{w}^T\mathbf{A}^{-1}\mathbf{w})\Delta t}$ tends to zero as τ tends to infinity. Hence, we have

$$\lim_{\tau\to\infty}e^{-\tau\mathbf{A}^{-1}\mathbf{w}\mathbf{w}^T\Delta t}=\mathbf{I}-\frac{\mathbf{A}^{-1}\mathbf{w}\mathbf{w}^T}{\mathbf{w}^T\mathbf{A}\mathbf{w}}. \tag{22}$$

Observe that this relation for the limit holds independent of Δt. On the other hand, as Δt tends to zero,

$$\lim_{\Delta t \to 0} e^{-\mathbf{A}^{-1}\mathbf{B}\Delta t} = \mathbf{I}. \tag{23}$$

Also, we have

$$\begin{aligned}\lim_{\tau\to\infty} e^{-\mathbf{A}^{-1}(\mathbf{B}+\tau\mathbf{w}\mathbf{w}^T)(\Delta t-s)} &= e^{-\mathbf{A}^{-1}\mathbf{B}(\Delta t-s)} \lim_{\tau\to\infty} e^{-\tau\mathbf{A}^{-1}\mathbf{w}\mathbf{w}^T(\Delta t-s)} \\ &= e^{-\mathbf{A}^{-1}\mathbf{B}(\Delta t-s)} \left(\mathbf{I} - \frac{\mathbf{A}^{-1}\mathbf{w}\mathbf{w}^T}{\mathbf{w}^T\mathbf{A}\mathbf{w}}\right).\end{aligned}$$

It follows that

$$\lim_{\Delta t\to 0} \lim_{\tau\to\infty} \int_0^{\Delta t} e^{-\mathbf{A}^{-1}(\mathbf{B}+\tau\mathbf{w}\mathbf{w}^T)(\Delta t-s)} \mathbf{A}^{-1}\mathbf{i}\, ds = 0. \tag{24}$$

Combining (19), (22), (23), and (24), the proof is complete. ∎

Observe that the limit (18) of Theorem 2 and that of (10) in Theorem 1 coincide when $\mu = 1$.

5. BREAKDOWN ON MULTIPLE ARCS

In this section, we consider breakdown on multiple arcs. This occurs when the limit in (18) yields an electric potential that violates the constraint (6) for a pair of adjacent centroids in the tessellation. Let $\mathbf{\Phi}^+(t_n)$ denote the limit in (18). Due to (11) in the case $\mu = 1$, we know that the left side of (6) vanishes for the index pair (j, k) and the potential $\mathbf{\Phi}^+(t_n)$. However, there may exist another pair of adjacent centroids, and associated index pair (l, m), for which the potential $\mathbf{\Phi}^+(t_n)$ violates the constraint (6). When this happens, we will simultaneously let σ tend to infinity on two different cube faces. Our procedure for determining the second face where we let σ tend to infinity is the following: Consider the convex combination $\mathbf{\Phi}^\lambda$ defined by

$$\mathbf{\Phi}^\lambda = (1-\lambda)\mathbf{\Phi}^n + \lambda\mathbf{\Phi}^+(t_n).$$

As λ moves from 0 to 1, the potential $\mathbf{\Phi}^\lambda$ moves from its present value $\mathbf{\Phi}^n$ toward the limit $\mathbf{\Phi}^+(t_n)$ that the potential is trying to achieve. Since $\mathbf{\Phi}^\lambda$ is a linear function of λ, it follows that $\mathbf{\Phi}_j^\lambda - \mathbf{\Phi}_k^\lambda$ is a linear function of λ that has magnitude hE_B at $\lambda = 0$, and that vanishes at $\lambda = 1$ (by Theorem 1 with $\mu = 1$). Thus for the breakdown arc (the arc connecting the centroids associated with j and k), the difference

$$\mathbf{\Phi}_j^\lambda - \mathbf{\Phi}_k^\lambda$$

is approaching 0 monotonically as λ moves from 0 to 1.

If $\mathbf{\Phi}^+(t_n)$ violates (6) for a pair of adjacent centroids, then we consider the first value of λ with the property that

$$\frac{\left|\mathbf{\Phi}_l^\lambda - \mathbf{\Phi}_m^\lambda\right|}{h} = E_B$$

for a pair of indices (l, m) associated with adjacent centroids in the tessellation. In numerical experiments, we observe typically that either l or m is equal to either j or k, and the breakdown moves to a cube adjacent to the original pair of cubes. We now let σ tend to infinity on both the face associated with the original pair (j, k) and the face associated with the new pair (l, m). If $\mathbf{v}$ denotes the vector whose entries are all zero except that $v_l = 1$ and $v_m = -1$, then we need to solve the equation

$$\mathbf{A}\dot{\mathbf{\Phi}} + (\mathbf{B} + \tau \mathbf{w}\mathbf{w}^T + \tau \mathbf{v}\mathbf{v}^T)\mathbf{\Phi} + \mathbf{i} = 0, \tag{25}$$

in the case that τ tends to infinity. If $\mathbf{U}$ is the matrix whose first column is $\mathbf{w}$ and whose second column is $\mathbf{v}$, it can be checked that

$$\mathbf{U}\mathbf{U}^T = \mathbf{w}\mathbf{w}^T + \mathbf{v}\mathbf{v}^T.$$

Hence, (25) takes the form:

$$\mathbf{A}\dot{\mathbf{\Phi}} + (\mathbf{B} + \tau \mathbf{U}\mathbf{U}^T)\mathbf{\Phi} + \mathbf{i} = 0. \tag{26}$$

THEOREM 3. *If* $\mathbf{A}$ *is a positive definite matrix and* $\mathbf{\Phi}(t, \tau)$ *denotes the solution to* (26) *starting from the initial condition* $\mathbf{\Phi}(t_n, \tau) = \mathbf{\Phi}^n$, *then we have*

$$\lim_{\Delta t \to 0} \lim_{\tau \to \infty} \mathbf{\Phi}(t_n + \Delta t, \tau) = \mathbf{\Phi}^n - \mathbf{A}^{-1}\mathbf{U}(\mathbf{U}^T\mathbf{A}^{-1}\mathbf{U})^{-1}\mathbf{U}^T\mathbf{\Phi}^n. \tag{27}$$

Proof. We use the same strategy used to prove Theorem 1; however, some care is needed since matrix products do not commute generally. In particular, the generalization of (21) is

$$(\mathbf{A}^{-1}\mathbf{U}\mathbf{U}^T)^\kappa = \mathbf{A}^{-1}\mathbf{U}(\mathbf{U}^T\mathbf{A}^{-1}\mathbf{U})^{\kappa-1}\mathbf{U}^T = \mathbf{A}^{-1}\mathbf{U}(\mathbf{U}^T\mathbf{A}^{-1}\mathbf{U})^{-1}(\mathbf{U}^T\mathbf{A}^{-1}\mathbf{U})^\kappa\mathbf{U}^T,$$

which leads to the relation

$$e^{-\tau \mathbf{A}^{-1}\mathbf{U}\mathbf{U}^T \Delta t} = \mathbf{I} + \mathbf{A}^{-1}\mathbf{U}(\mathbf{U}^T\mathbf{A}\mathbf{U})^{-1}\left(e^{-\tau(\mathbf{U}^T\mathbf{A}^{-1}\mathbf{U})\Delta t} - \mathbf{I}\right)\mathbf{U}^T.$$

Since $\{j, k\} \neq \{l, m\}$, it follows that the columns of $\mathbf{U}$ are linearly independent. Since $\mathbf{A}$ is positive definite, $\mathbf{U}^T\mathbf{A}^{-1}\mathbf{U}$ is positive definite, and $e^{-\tau(\mathbf{U}^T\mathbf{A}^{-1}\mathbf{U})\Delta t}$ tends to zero as τ tends to infinity. Hence, we have

$$\lim_{\tau \to \infty} e^{-\tau \mathbf{A}^{-1}\mathbf{U}\mathbf{U}^T \Delta t} = \mathbf{I} - \mathbf{A}^{-1}\mathbf{U}(\mathbf{U}^T\mathbf{A}\mathbf{U})^{-1}\mathbf{U}^T.$$

Finally, we multiply by $\mathbf{\Phi}^n$ to complete the proof. ∎

COROLLARY 1. *If* $\mathbf{\Phi}^+$ *denotes the limit appearing on the right side of* (27), *then* $\Phi_j^+ = \Phi_k^+$ *and* $\Phi_l^+ = \Phi_m^+$.

Proof. Multiplying (27) by $\mathbf{U}^T$, we see that $\mathbf{U}^T\mathbf{\Phi}^+ = 0$. Since the columns of $\mathbf{U}$ are $\mathbf{w}$ and $\mathbf{v}$, the relation $\mathbf{U}^T\mathbf{\Phi}^+ = 0$ implies that $\mathbf{w}^T\mathbf{\Phi}^+ = 0$ and $\mathbf{v}^T\mathbf{\Phi}^+ = 0$. By the definition of $\mathbf{v}$ and $\mathbf{w}$, $\Phi_j^+ = \Phi_k^+$ and $\Phi_l^+ = \Phi_m^+$. ∎

Observe that if either l or m is equal to either j or k, then the discharge is moving to an adjacent centroid, and by Corollary 1, $\Phi_j^+ = \Phi_k^+ = \Phi_l^+ = \Phi_m^+$. Thus the discharge is equilibrating the potential throughout the breakdown region.

Multiple breakdowns continue in this same way. In each step, we form a convex combination of the current potential $\mathbf{\Phi}^n$ and the limiting potential $\mathbf{\Phi}^+$ obtained from Theorem 3. If the limit satisfies the breakdown condition

$$\frac{|\Phi_a^+ - \Phi_b^+|}{h} \leq E_B \tag{28}$$

for each pair of adjacent centroids in the lattice of centroids, then the discharge is complete; the potential jumps from $\mathbf{\Phi}^n$ to $\mathbf{\Phi}^+$, and it continues to evolve according to (5). On the other hand, if (28) is violated for an adjacent pair of centroids in the tessellation, then we determine the first value of λ and the associated indices a and b for which

$$\frac{\left|\Phi_a^\lambda - \Phi_b^\lambda\right|}{h} = hE_B. \tag{29}$$

Another column is added to the matrix $\mathbf{U}$ where each entry in the new column is zero except for a $+1$ and -1 in positions a and b. Again, the solution to (26) has the limit (27). The proof of Theorem 3 when $\mathbf{U}$ has more than two columns hinges on the observation that the columns of $\mathbf{U}$ are linearly independent. This independence is due to the fact that $\mathbf{U}$ is the node-arc incidence matrix associated with the graph of the centroids connected by breakdown (see [1, Theorem 11.9] for the relevant result).

In summary, the lightning discharge proceeds in the following way:

(1) If $\mathbf{U}$ is the node-arc incidence matrix associated with the current breakdown region, and if $\mathbf{\Phi}^+$ denotes the limit (27) of Theorem 2, then we check whether (28) holds for each pair of centroids. If (28) is satisfied, then the breakdown stops, the potential jumps from $\mathbf{\Phi}^n$ to $\mathbf{\Phi}^+$, and the potential continues to evolve according to (5). If (28) is violated for a pair of centroids, then proceed to step (2).

(2) Determine the first value of λ between 0 and 1 with the property that (29) holds for two adjacent centroids in the tessellation. Augment $\mathbf{U}$ with an additional column where every entry in that column is 0 except for a $+1$ and -1 in positions a and b. Return to step (1).

By Corollary 1, and its generalization to an arbitrary number of columns in $\mathbf{U}$, we know that after the discharge is complete, the potential is constant along the arcs associated with connected components of the breakdown region. Moreover, if the Earth is treated as a perfect conductor and if a branch of the breakdown path reaches the surface of the Earth, then the components of $\mathbf{\Phi}$ associated with the path reaching the Earth all vanish.

An example of a cloud to ground flash from [4] appears in Fig. 1. In performing this simulation, it was assumed that there were three charge centers along the z-axis, a small positive center at the base of the cloud (2 km), and larger negative and positive centers at 5 and 10 km, respectively. Since the charge is placed along the z-axis, the potential is cylindrically symmetric. The potential was computed using a cylindrical coordinate system and a graded mesh. The model domain had a height and radius of 100 km. The mesh spacing for the region depicted in Fig. 1 is about 313 m in the radial direction and 192 m in the vertical direction.

The breakdown process illustrated in Fig. 1 involves 42 steps. In each step, we let σ tend to infinity somewhere in the domain, and we reevaluate the potential to determine whether $\|\mathbf{E}\|_\infty$ has reached E_B elsewhere in the domain. The five frames of Fig. 1 show the breakdown region after steps 19, 26, 32, 38, and 42, respectively. The breakdown initiates

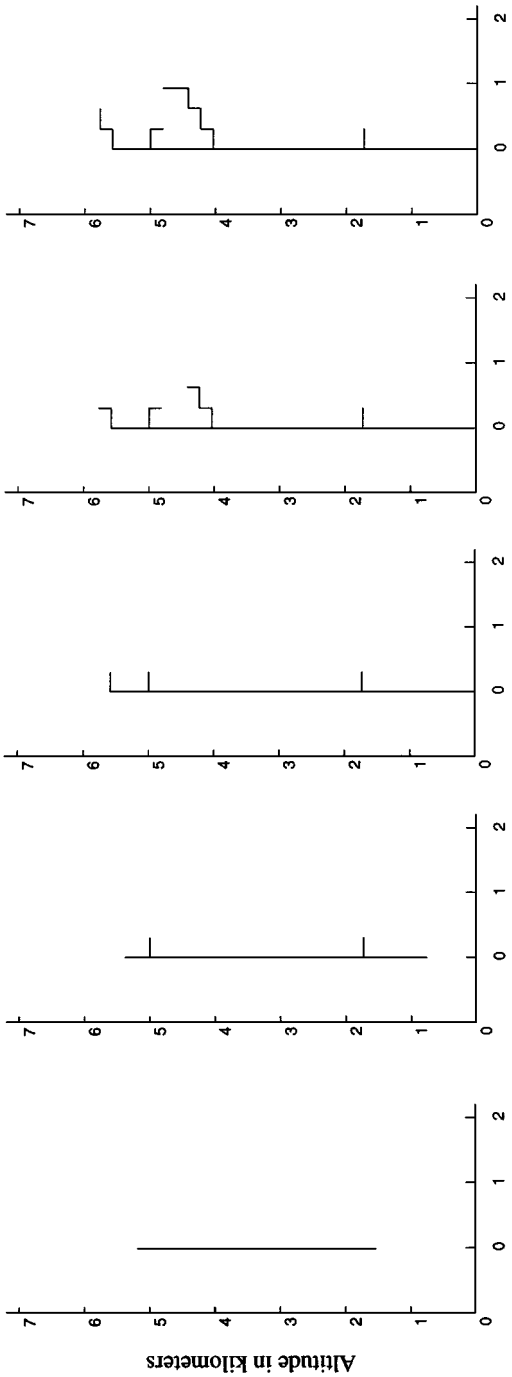

FIG. 1. A cloud to ground flash from [4] with generators on the z-axis.

at an altitude around 3.3 km, and progresses both downward and upward. The first frame of Fig. 1 shows the breakdown region during this startup period. Horizontal fingers appear in the second frame, while in the next frame, the breakdown reaches the ground. In the final two frames, the breakdown fingers outward, primarily in a horizontal direction. Each step in the breakdown process is either horizontal or vertical since breakdown in our model is initiated when $\|\mathbf{E}\|_\infty = E_B$. By changing from the sup-norm to the Euclidean norm, the stair-like breakdown path can be smoothed out.

Although one may think of Fig. 1 as representing a slow motion picture of the lightning flash generated by our model, the actual elapsed time for the breakdown process is zero. That is, we view the entire process as taking place instantaneously (relative to the time step Δt of (8), which can be on the order 0.1 second). At the end of the breakdown process, we obtain a region of space where ϕ vanishes since the lightning channel has reached the ground where the potential is zero (the Earth is treated as a perfect conductor in the simulation). The breakdown process has led to a new potential for which the constraint $\|\mathbf{E}\|_\infty \le E_B$ is satisfied with strict inequality throughout the model domain.

6. DISCUSSION

The formula obtained in Theorem 3 for the change in the potential associated with a series of breakdown arcs for the continuous-in-time equation is exactly the same formula obtained in [3, 4] using the backward Euler scheme for the time integration. When we took τ to infinity in the backward Euler scheme, the effect on errors was not clear. By Theorem 3, the jumps in the potential associated with the continuous time process and with the backward Euler time discretization are identical.

By Theorem 3, the change in the potential associated with the lightning discharge is

$$\mathbf{A}^{-1}\mathbf{U}(\mathbf{U}^T\mathbf{A}^{-1}\mathbf{U})^{-1}\mathbf{U}^T\mathbf{\Phi}^n.$$

Since $\mathbf{U}$ is a node-arc incidence matrix with a $+1$ and -1 in each column corresponding to the arcs associated with the breakdown, and since the difference of two components of $\mathbf{\Phi}^n$ is roughly proportional to the electric field between the associated centroids, it follows that $\mathbf{U}^T\mathbf{\Phi}^n$ is a vector whose components are roughly proportional to the original electric field (before breakdown) evaluated along the ensuing breakdown path. The matrix $\mathbf{A}^{-1}\mathbf{U}(\mathbf{U}^T\mathbf{A}^{-1}\mathbf{U})^{-1}$ shows how the breakdown process and the original electric field (before breakdown) interact to change the potential (and the electric field) throughout the entire domain. In essence, the formula of Theorem 3 provides the mathematical analogue of the experimental observations of Williams *et al.* cited earlier.

REFERENCES

1. R. K. Ahuja, T. L. Magnanti, and J. B. Orlin, *Network Flows: Theory, Algorithms, and Applications* (Prentice-Hall, Englewood Cliffs, NJ, 1993).
2. W. W. Hager, Updating the inverse of a matrix, *SIAM Rev.* **31**, 221 (1989).
3. W. W. Hager, J. S. Nisbet, and J. R. Kasha, The evolution and discharge of electric fields within a thunderstorm, *J. Comput. Phys.* **82**, 193 (1989).
4. W. W. Hager, J. S. Nisbet, J. R. Kasha, and W.-C. Shann, Simulations of electric fields within a thunderstorm, *J. Atmospheric Sci.* **46**, 3542 (1989).

5. J. H. Helsdon, Jr. and R. D. Farley, A numerical modeling study of a Montana thunderstorm. 1. Model results versus observations involving nonelectrical aspects, *J. Geophys. Res.* **92**, 5645 (1987).
6. J. H. Helsdon, Jr. and R. D. Farley, A numerical modeling study of a Montana thunderstorm. 2. Model results versus observations involving electrical aspects, *J. Geophys. Res.* **92**, 5661 (1987).
7. J. H. Helsdon, Jr., R. D. Farley, and G. Wu, Lightning parameterization in a storm electrification model, in *1988 Proceedings, International Conference on Atmospheric Electricity*, p. 849.
8. J. H. Helsdon, Jr., G. Wu, and R. D. Farley, An intracloud lightning parameterization scheme for a storm electrification model, *J. Geophys. Res.* **97**, 5865 (1992).
9. T. C. Marshall, M. P. McCarthy, and W. D. Rust, Electric field magnitudes and lightning initiation in thunderstorms, *J. Geophys. Res.* **100**, 7097 (1995).
10. T. C. Marshall and W. D. Rust, Electric field soundings through thunderstorms, *J. Geophys. Res.* **96**, 22,297 (1991).
11. L. Niemeyer, L. Pietronero, and H. J. Wiesmann, Fractal dimension of dielectric breakdown, *Phys. Rev. Lett.* **52**, 1033 (1984).
12. K. Norville, M. Baker, and J. Latham, A numerical study of thunderstorm electrification: Model development and case study, *J. Geophys. Res.* **96**, 7463 (1991).
13. N. I. Petrov and G. N. Petrova, Physical mechanism for intracloud lightning discharges, *Tech. Phys.* **38**, 287 (1993).
14. L. Pietronero and H. J. Wiesmann, Stochastic model for dielectric breakdown, *J. Statist. Phys.* **36**, 909 (1984).
15. C. I. Richman, Fractal geometry of lightning strokes, in *MILCOM 90* (IEEE, New York, 1990).
16. B. M. Smirnov, The properties and the nature of ball lightning, *Phys. Rep.* **152**, 177 (1987).
17. R. Solomon and M. Baker, A one-dimensional lightning parameterization, *J. Geophys. Res.* **101**, 14,983 (1996).
18. M. A. Uman, *The Lightning Discharge* (Academic Press, Orlando, 1987).
19. E. R. Williams, C. M. Cooke, and K. A. Wright, Electrical discharge propagation in and around space charge clouds, *J. Geophys. Res.* **90**, 6059 (1985).
20. T. A. Witten, Jr. and L. M. Sander, Diffusion-limited aggregation, a kinetic critical phenomenon, *Phys. Rev. Lett.* **47**, 1400 (1981).
21. C. L. Ziegler and D. R. MacGorman, Observed lightning morphology relative to modeled space charge and electric field distributions in a tornadic storm, *J. Atmospheric Sci.* **51**, 833 (1994).
22. C. L. Ziegler, D. R. MacGorman, J. E. Dye, and P. R. Ray, A model evaluation of noninductive graupel-ice charging in the early electrification of a mountain thunderstorm, *J. Geophys. Res.* **96**, 12,833 (1991).